Assignment of the Zinc Ligands in RsrA, a Redox-Sensing ZAS Protein from *Streptomyces coelicolor*†

Konrad Zdanowski,‡ Phillip Doughty,§ Piotr Jakimowicz,|| Liisa O'Hara,§ Mark J. Buttner,|| Mark S. B. Paget,§ and Colin Kleanthous*,‡

Department of Biology (Area 10), University of York, P.O. Box 373, York YO10 5YW, U.K., Department of Biochemistry, School of Life Sciences, University of Sussex, Falmer, Brighton BN1 9QG, U.K., and Department of Molecular Microbiology, John Innes Centre, Norwich NR4 7UH, U.K.

Received April 12, 2006; Revised Manuscript Received May 15, 2006

ABSTRACT: ZAS proteins are widespread bacterial zinc-containing *a*nti-*s*igma factors that regulate the activity of sigma factors in response to diverse cues. One of the best characterized ZAS proteins is RsrA from *Streptomyces coelicolor*, which responds to disulfide stress. Zn−RsrA binds and represses the transcriptional activity of σ^R in the reducing environment of the cytoplasm but undergoes reversible, intramolecular disulfide bond formation during oxidative stress. This expels the single metal ion and causes dramatic structural changes in RsrA that result in its dissociation from σ^R, leaving the sigma factor free to activate the transcription of antioxidant genes. We showed recently that Zn^{2+} serves a critical role in modulating the redox activity of RsrA thiols but uncertainty remains as to how the metal ion is coordinated in RsrA and related ZAS proteins. Using a combination of random and site-specific mutagenesis with zinc K-edge extended X-ray absorption fine structure (EXAFS) spectroscopy, we have assigned unambiguously the metal ligands in RsrA, thereby distinguishing between the different ligation models that have been proposed. The data show that the zinc site in RsrA is comprised of Cys11, His37, Cys41, and Cys44. Three of these residues are part of a conserved ZAS-specific sequence motif ($H^{37}xxxC^{41}xxC^{44}$), with the fourth ligand, Cys11, found in a subset of ZAS proteins. Cys11 and Cys44 form the trigger disulfide in RsrA, explaining why the metal ion is expelled during oxidation. We discuss these data in the context of redox sensing by RsrA and the sensory mechanisms of other ZAS proteins.

A consequence of oxygen being the ultimate electron acceptor in respiration is the generation of reactive oxygen species (ROS), such as superoxide (O_2^-) and hydrogen peroxide (H_2O_2), as byproducts, exposing biological systems to "oxidative stress". ROS are highly damaging since they can inactivate proteins, damage DNA, and perturb membrane integrity, with long-term exposure implicated in aging, cancer, and neurodegenerative disease (*2*, *3*). To reap the benefits of an oxygen-rich existence, while minimizing exposure to oxidative stress, all aerobic organisms have evolved mechanisms to detect and counteract its effects. One of the consequences of H_2O_2 production, for example, is the posttranslational modification of protein thiols, which have the potential to alter protein function. To combat thiol oxidation, cells maintain a reducing cytoplasm, accomplished by having millimolar concentrations of low molecular weight thiol buffers such as glutathione (in *Escherichia coli*) or mycothiol (in actinomycetes such as *Streptomyces coelicolor*). In addition, conserved oxidoreductases, thioredoxin and glutaredoxin, reduce disulfide bonds through thiol−disulfide exchange reactions that are ultimately driven by the reducing potential of NADPH (*4*).

Notwithstanding this armory of antioxidants, unwanted disulfide bonds can form within and between cytoplasmic proteins. Described by Åslund and Beckwith as "disulfide stress" (*5*), this signifies a change in the overall thiol−disulfide redox balance, which can be distinct from "peroxide stress". A number of systems have now been identified where such stresses activate the transcription of antioxidant genes, the elevated products of which reestablish redox homeostasis. A central feature of such systems is thiol-based regulatory switches that transduce oxidative stress signals into coordinated cellular responses, in other words, where the very reactivity of cysteine thiols that leaves them vulnerable to oxidation is adapted as a signaling device (*6*, *7*). In general, these switches comprise "sensor cysteines" within regulatory proteins that are reversibly modified (for example, to sulfenic acids and/or disulfide bonds), resulting in changes in protein conformation and alterations in gene expression, either directly or indirectly.

Thiol-based regulatory switch proteins can be divided into two categories: those requiring metal ions and those with no metal involvement. In the latter category, OxyR is the archetypal example found in bacteria. OxyR is a tetrameric transcription factor from *E. coli* that is inactive in its reduced state and is activated directly by H_2O_2. H_2O_2 induces an intramolecular disulfide bond via an intermediate sulfenic

† This work was funded by The Wellcome Trust and the Biotechnology and Biological Sciences Research Council of the U.K.

* To whom correspondence should be addressed. Tel: +44-1904-328820. Fax: +44-1904-328825. E-mail: ck11@york.ac.uk.

‡ University of York.

§ University of Sussex.

|| John Innes Centre.

10.1021/bi060711v CCC: $33.50
Published on Web 06/15/2006

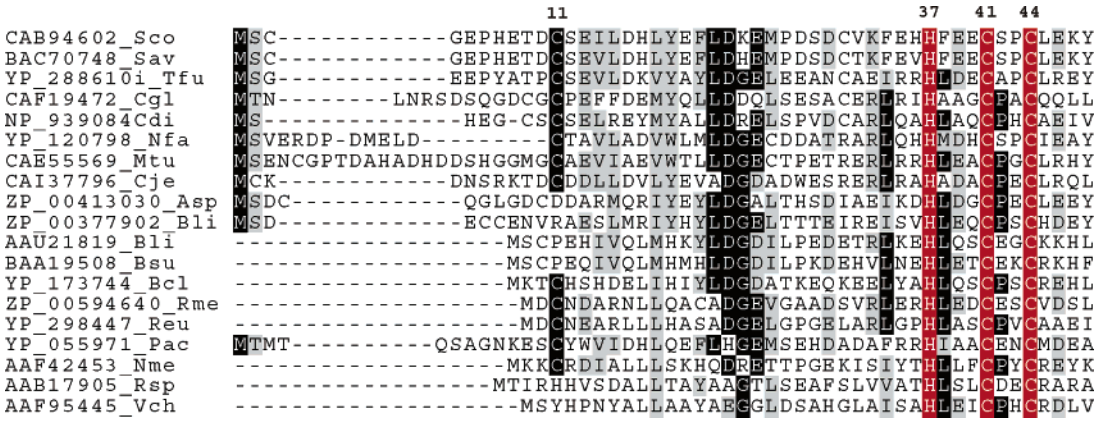

FIGURE 1: N-Terminal amino acid sequence alignments of the ZAS protein family. Highlighted in red are the conserved motif residues that denote the ZAS family. Key: *S. coelicolor* A3(2), RsrA, CAB94602; *Streptomyces avermitilis* MA-4680, BAC70748; *Thermobifida fusca* YX, YP_288610; *Corynebacterium glutamicum* ATCC 13032, CAF19472; *Corynebacterium diphtheriae* NCTC 13129, CAF19472; *Nocardia farcinica* IFM 10152, YP_120798; *Mycobacterium tuberculosis* H37Rv, CAE55569; *Corynebacterium jeikeium* K411, CAI37796; *Arthrobacter* sp. FB24, ZP_00413030; *Brevibacterium linens* BL2, ZP_00377902; *Bacillus licheniformis* ATCC 14580, AAU21819; *B.subtilis*, RsiW, BAA19508; *Bacillus clausii* KSM-K16, YP_173744; *Ralstonia metallidurans* CH34, ZP_00594640; *Ralstonia eutropha* JMP134, YP_298447; *Propionibacterium acnes* KPA171202, YP_055971; *Neisseria meningitidis* MC58, AAF42453; *Rh. sphaeroides*, ChrR, AAB17905; *Vibrio cholerae* N16961, AAF95445.

acid at a sensor cysteine (*8*−*10*). Significant restructuring of the protein alters its DNA-binding properties, leading to transcriptional activation of >20 antioxidant genes, including *grxA*, encoding glutaredoxin 1. Activated OxyR is subsequently a substrate for reduction by glutaredoxin 1, thereby creating a redox homeostasis loop (*8*).

Metal ions are increasingly being found in redox sensing systems and, in particular, zinc (*7*, *11*). Although not redox active, Zn^{2+} can bind to sensor cysteines and modulate their reactivity toward oxidants (*1*, *12*). Indeed, within both mammalian and bacterial systems there is an intimate link between zinc metabolism and redox homeostasis (*13*). One of the first redox-sensing, zinc-based transcriptional regulators to be identified was RsrA from the Gram-positive soil bacterium *S. coelicolor*. The cellular response to disulfide stress in *S. coelicolor* is under the control of the ECF sigma factor σ^R, which has a regulon of at least 30 genes and includes those encoding thioredoxin and thioredoxin reductase (*14*, *15*). σ^R, however, contains no cysteines and so is not a direct sensor of disulfide stress. This is the role of its anti-sigma factor, RsrA, a protein of 105 amino acids and 7 cysteines. In its reduced state RsrA binds a single zinc atom (Zn−RsrA) and forms a 1:1 complex with σ^R that suppresses its transcriptional activity (*16*). Although up to three disulfide bonds can form in RsrA, a single "trigger disulfide", involving residues 11 and 44, is sufficient to drive the expulsion of the bound metal ion and to cause a change in protein conformation (*1*, *11*). This in turn disrupts the σ^R−RsrA complex, releasing σ^R to bind RNA polymerase. Both *sigR* and *rsrA* genes are under σ^R control, thereby amplifying the response, and the homeostatic loop is closed when oxidized RsrA is reduced by thioredoxin, allowing it to reassociate with σ^R (*16*).

RsrA was the first-described member of the Zn-containing anti-sigma factor (ZAS)[1] family of proteins (*17*). ZAS genes are normally found downstream of their target ECF sigma factor genes, and ZAS proteins show only weak sequence conservation, identified primarily by an invariant HxxxCxxC sequence motif in the N-terminal σ-binding domain (Figure 1). The C-terminal region of ZAS proteins varies widely in both sequence composition and length. For example, although RsrA and the anti-σ^W factor RsiW in *Bacillus subtilis* show similarity in the N-terminal ~60 amino acids, RsiW has a C-terminal extension that includes a membrane-spanning helix and an extracytoplasmic ~100 amino acid domain (*18*).

Although one or more of the zinc-coordinating cysteine ligands in RsrA have been implicated in redox sensing, it seems clear that not all ZAS proteins respond to oxidative stress. For example, although RsiW contains the equivalent cysteine residues that have been implicated in redox sensing in RsrA, the activity of σ^W in *B. subtilis* is not induced by oxidants but by alkaline stress and by compounds that inhibit cell wall synthesis (J. D. Helmann, personal communication) (*19*, *20*). In *Rhodobacter sphaeroides*, the ZAS protein ChrR binds zinc and is involved in a redox-sensing pathway but appears to use a mechanism distinct from that of RsrA (*21*, *22*). ChrR controls σ^E, which activates the expression of ~180 genes (~60 operons) in response to singlet oxygen formed during aerobic photosynthesis (*22*). Importantly, oxidants such as diamide and hydrogen peroxide that inactivate RsrA do not inactivate ChrR (T. J. Donohue, personal communication) (*22*).

As a step toward understanding the differential reactivity of ZAS anti-sigma factors to oxidants, the primary aim of the work described herein was to determine how the Zn^{2+} ion in RsrA is coordinated, using a combination of mutagenesis and spectroscopy.

MATERIALS AND METHODS

Strains and Plasmids. S. coelicolor M600 is a wild-type prototrophic plasmid-free strain (*23*). *S. coelicolor* J2146 is a derivative of M600 with the *sigR* and *rsrA* genes replaced by a hygromycin resistance cassette (*17*). *E. coli* ET12567

[1] Abbreviations: $RsrA^{C11,C41,C44}$, mutant of RsrA that has the four nonessential cysteines (Cys3, Cys31, Cys61, and Cys62) substituted for alanine; RsrA H37A, mutant of RsrA that has His37 substituted for alanine; EXAFS, extended X-ray absorption fine structure; ZAS, zinc-binding anti-sigma factor; ECF, extracytoplasmic sigma factor; DTNB, 5,5′-dithiobis(2-nitrobenzoic acid).

(pUZ8002) is defective in DNA methylation systems and is used as a helper strain for *E. coli*−*Streptomyces* conjugations (*24*). pIJ6656 contains the *sigR*−*rsrA Bcl*I−*Bam*HI fragment, including the upstream regulatory region, cloned in pBluescript II SK+ (*17*). pSET152 is an *E. coli*−*Streptomyces* conjugative vector that integrates into the ϕC31 phage attachment site (*25*).

Plasmid Constructions. pSX202 is an integrative plasmid that contains the *sigR*−*rsrA*/*neo* fusion. The *neo* gene was amplified from pIJ487 (*26*), incorporating an N-terminal *Bam*HI site and a C-terminal *Xba*I site, and subcloned downstream of *rsrA* in *Bam*HI−*Xba*I-digested pIJ6656. Inverse PCR-mediated site-directed mutagenesis was used to create an *rsrA/neo* translational fusion (pSX201), replacing the *rsrA* stop codon and *neo* start codon, along with the intervening DNA, with a *Spe*I restriction site. This allows the subsequent removal of *neo* from pSX202 by *Spe*I and *Xba*I digestion, filling in the recessed 3′ ends, and self-ligation, generating an *rsrA* stop codon. The *sigR*−*rsrA/neo* fusion was isolated as an *Eco*RV−*Xba*I fragment and subcloned into pSET152 to generate pSX202.

Mutagenesis of RsrA. Random mutagenesis of pSX202, which carries the *sigR*−*rsrA* region, was performed using hydroxylamine. pSX202 (10 μg) was incubated in mutagenesis buffer [50 mM KH_2PO_4/K_2HPO_4, 5 mM EDTA, 0.5 M hydroxylamine hydrochloride (freshly prepared in 0.5 M NaOH)] for 2 h at 70 °C. The mutagenized DNA was ethanol-precipitated and then used to transform *E. coli* ET12567 (pUZ8002) to generate a library of ∼10000 transformants. The library was pooled and used to conjugate with *S. coelicolor* J2146 as described (*23*). White or pale gray exconjugants were chosen for further phenotypic analysis. The level of conferred kanamycin resistance was determined by replica-plating exconjugants to kanamycin-containing minimal agar. White mutants that exhibited a level of kanamycin resistance equal to or higher than that of J2146 (pSX202) were analyzed further by PCR, amplifying and sequencing the *sigR*−*rsrA* coding regions.

Site-specific mutagenesis was used to change the H37 codon to an alanine in different genetic contexts for in vivo and in vitro analyses. For in vivo analyses the H37 codon (CAC) was changed to alanine (GCC) in pIJ6656 by inverse PCR-mediated site-directed mutagenesis (*27*). The *sigR*−*rsrA*^{H37A} region was subcloned as an *Eco*RV−*Bam*HI fragment into pSET152 to generate pSX112^{H37A} and then conjugated into *S. coelicolor* J2146. For in vitro analysis, the mutagenesis was repeated using a derivative of pBluescript II SK+ that contained the *rsrA* reading frame as an *Nde*I−*Bam*HI fragment and then subcloned into pET15b (Novagen).

Disulfide Reductase Assay. Disulfide reductase assays were performed with crude cell extracts using DTNB as the disulfide-containing substrate, as described by Paget et al. (*14*). Protein concentration was measured using the Bradford assay, and assays were performed three times with independent cultures. Cells extracts were prepared from mid-late exponential phase liquid cultures as described (*17*). Disulfide stress was imposed by the addition of 0.5 mM diamide for 45 min prior to harvesting.

Protein Preparation. RsrA and σ^R were expressed and purified from *E. coli* BL21(DE3)pLysS and quantitated as described previously (*14*, *16*, *28*). Two site-specific mutants of RsrA were also used in these studies: RsrA H37A and RsrA^{C11,C41,C44}, the latter in which cysteines C11, C41, and C44 are unaltered but the remaining four cysteines (C3, C31, C60, and C61) were substituted for alanine. During preparation of Zn-loaded RsrA, overexpressing bacteria were supplemented with 50 μM $ZnCl_2$ (*1*). Complexes of RsrA and its two mutants with σ^R were monitored by native gel electrophoresis (12%). The presence of zinc in all RsrA protein preparations was established using the spectrophotometric PAR assay, as previously described (*1*).

EXAFS Data Collection and Analysis. Purified proteins were concentrated using centricons (Amicon) to 1.5−2.5 mM in 50 mM Tris-HCl, pH 7.5, containing 200 mM NaCl and 20 mM DTT. These consisted of wild-type Zn−RsrA, Zn−RsrA H37A, Zn−RsrA^{C11,C41,C44}, and wild-type Zn−RsrA bound to σ^R. Fluorescence EXAFS data were collected using the 16.5 beam line at the Synchrotron Radiation Source at Daresbury (Cheshire, U.K.), using a vertically focusing mirror and a sagittally bent focusing Si(220) double crystal monochromator detuned to 80% transmission to minimize harmonic contamination. The incident X-ray intensity, I_o, was measured with an ion chamber filled with a mixture of Ar and He gases, and a 30-element Ge solid-state detector with high count−rate electronics was used to collect the X-ray fluorescence signal. The Zn K-absorption edge of each protein preparation was recorded using a liquid nitrogen cryostat. To improve the signal-to-noise ratio, multiple scans were collected for each sample; 8 scans were collected for each Zn-bound RsrA protein and 14 scans for the Zn−RsrA−σ^R complex, which was at a lower concentration relative to the other samples. All EXAFS data were analyzed using the Daresbury Laboratory suite of programs. The calibration was carried out using the program EXCALIB, background subtraction was performed using EXSPLINE (*29*), and simulations of the background-subtracted, k^3-weighted raw EXAFS data were obtained with EXCURV98 (*30*), applying fast curved wave theory (*31*). The phase shifts employed were calculated using Hedin−Lundqvist exchange and correlation potentials (*32*).

RESULTS

His37 Is Required for RsrA Activity in Vivo. Previously, we used site-directed mutagenesis to demonstrate the key in vivo and in vitro importance of three out of seven RsrA cysteine residues for RsrA function (Cys11, Cys41, and Cys44) (*17*). To better understand the σ^R−RsrA interaction, we set up a random in vivo screen to isolate new *sigR* or *rsrA* mutants defective in this interaction. The complete deletion of *rsrA* leads to constitutive σ^R activity and a distinctive white (Whi) phenotype caused by the inhibition of sporulation (*17*). The Whi phenotype is probably caused by competition between high levels of σ^R and a sporulation sigma factor, which ultimately prevents the formation of a spore-specific gray pigment (*17*). Therefore, mutations that prevent the interaction of σ^R and RsrA, but that retain functional σ^R, should exhibit a Whi phenotype. To screen against frame-shift and premature translation termination mutations in *rsrA*, the C-terminus of the *rsrA* open reading frame was translationally fused to the entire *neo* gene, which encodes the aminoglycoside phosphotransferase from Tn5 and confers kanamycin resistance on *S. coelicolor*. We rationalized that RsrA is likely to retain function even with

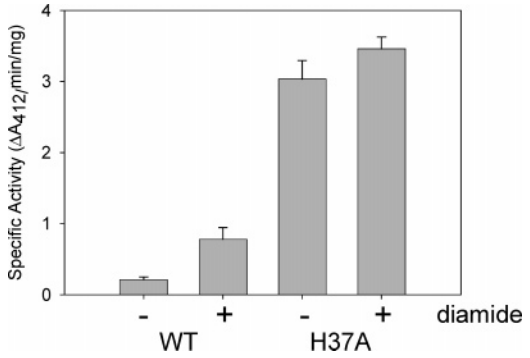

FIGURE 2: Disulfide reductase assay in J2146 (pSX112) (WT) and J2146 (pSX112^{H37A}) (H37A) before and after diamide treatment. Strains were grown in NMMP liquid medium to mid-late exponential phase and exposed to 0.5 mM diamide for 45 min where appropriate. Disulfide reductase activity in cell extracts was measured following the reduction of DTNB at 412 nm. Data are the mean of three independent experiments, and standard deviation is indicated.

a C-terminal translational fusion since many other ZAS anti-sigma factors (but not RsrA) have large C-terminal extensions that are thought to be involved in sensing specific signals (Figure 1) (*16*). Indeed, the *rsrA*/*neo* fusion was found to be active, as judged by the introduction of *sigR*−*rsrA*/*neo* (carried on the integrative plasmid pSET152) into the *S.* coelicolor J2146 [Δ(*sigR*−*rsrA*)::*hyg*]. pSX202 restored diamide resistance to J2146 and conferred kanamycin resistance at a level ∼10-fold higher (∼70 μg/mL) than the negative control (pSET152), indicating that both *sigR* and *rsrA* were expressed. Furthermore, sporulation was not affected, implying that the *rsrA/neo* fusion functioned as an anti-sigma factor. pSX202 was mutagenised by in vitro treatment with hydroxylamine, followed by its introduction into *S. coelicolor* J2146 by conjugation. White exconjugants that maintained levels of kanamycin resistance equal or higher than J2146 (pSX202) were identified and the corresponding *sigR*−*rsrA* regions sequenced. In an initial screen of approximately 10000 colonies 18 putative mutants were screened by sequencing and 8 contained mutations in RsrA. The majority of these (6/8) caused the conversion of His37 to phenylalanine (F), either by a single (C109T) or by double (C109T, C111T) nucleotide substitutions. The remaining two mutations (at residues 18 and 22) will be discussed elsewhere. To confirm the importance of His37, site-directed mutagenesis was used to convert the His37 codon to alanine. The *rsrA* H37A allele along with the coupled upstream *sigR* gene was introduced into J2146 on the integrative plasmid pSX112^{H37A}. As with the H37F mutations, the pSX112^{H37A} exconjugants exhibited a white phenotype, suggesting increased levels of σ^R. To confirm this, disulfide reductase assays were performed. The σ^R−RsrA system controls the expression of the thioredoxin reductase system as well as several other putative thiol−disulfide reductase pathways (*15*). Thus, disulfide stress induced by the thiol-specific oxidant diamide leads to 4-fold increased disulfide reductase activity, *sigR* null mutants have low uninducible levels, and *rsrA* null mutants exhibit high, uncontrolled levels (*14*, *17*). J2146 (pSX112^{H37A}) yielded 10-fold higher basal levels of disulfide reductase compared to J2146 (pSX112), and unlike the case for J2146 (pSX112), levels were not induced upon treatment with diamide (Figure 2). These data indicate that the *rsrA* H37A allele is essentially inactive and support the importance of His37 in RsrA function beyond its mere conservation within the HxxxCxxC motif.

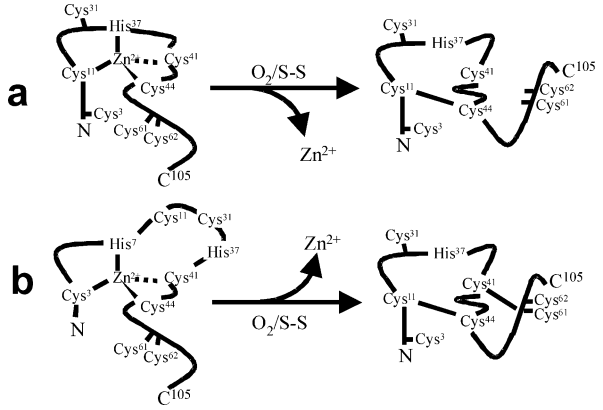

FIGURE 3: Models for the single zinc site in RsrA. (a) Model proposed by Li et al. (*1*). (b) Model proposed by Bae et al. (*33*). In both models the first disulfide bond to form in oxidized RsrA is that between Cys11 and Cys44, resulting in the loss of the metal ion. Bae et al. also identified a subsequent disulfide between Cys41 and Cys61. The models differ as to the identity of the four metal ligands. See text for details.

EXAFS Spectroscopy of Zn−*RsrA and Assignment of the Metal-Chelating Ligands.* Key to understanding how Zn−RsrA responds to disulfide stress is the coordination chemistry of the metal ion, which is expelled during protein oxidation and which in the reduced protein modulates thiol reactivity. Currently, no structures have been published for any ZAS protein, and although the ZAS motif is conserved, there is dispute as to how the zinc ion is chelated. Two models have been presented for its coordination chemistry (Figure 3). Bae et al. proposed a model, based on mutational and metal analysis data, that predicts Cys3, His7, Cys41, and Cys44 to be the metal ligands, implying that only two of the three ZAS motif residues in RsrA ($H^{37}xxxC^{41}xxC^{44}$) are involved in metal coordination (*33*). By contrast, we have suggested that the metal site is composed of all three ZAS motif residues, with Cys11 being the fourth metal ligand (*1*, *17*). This was based largely on in vivo and in vitro analysis of RsrA cysteine mutants, with the involvement of His37 a prediction stemming from its conservation in the ZAS motif. The data presented here lend support to this contention since mutations at His37 are recovered from random screens for RsrA mutants defective in anti-sigma factor activity in vivo. In summary, the two models that have been proposed for metal ion chelation in RsrA have only two of the four potential Zn^{2+} ligands in common, Cys41 and Cys44. Both of these residues have also been implicated in metal binding in another ZAS protein, ChrR from *Rh. sphaeroides* (*21*), a point we return to below.

To differentiate between the different metal-ligation and oxidation models, we used zinc K-edge EXAFS spectroscopy in combination with site-directed mutagenesis to assign the metal-coordinating residues of RsrA. The mutants selected were based on our previous model of the putative metal-binding site along with mutational data reported herein. Specifically, we prepared RsrA in which all but the three cysteines implicated in metal coordination by Paget et al. (*17*) and Li et al. (*1*) were mutated to alanine (RsrA^{C11,C41,C44}). This mutant is responsive to disulfide-induced stress using diamide in vivo and reversibly inhibits σ^R activity in vitro (*17*). In addition, a further mutant was examined in which

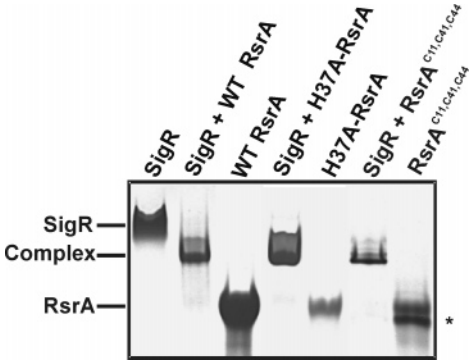

FIGURE 4: 12% native gel showing that Zn−RsrA and its two mutants (Zn−RsrA H37A, Zn−RsrA^{C11,C41,C44}) form complexes with Sig^R. The asterisk indicates the RsrA breakdown product. The concentration of the proteins loaded onto the gel varied between 2 and 10 nM.

only His37 was mutated to alanine. All proteins were purified as described previously from overexpressing strains of *E. coli* BL21(DE3)pLysS in which the growth medium was supplemented with $ZnCl_2$ (50 μM). The metal content of all proteins analyzed by EXAFS (Zn−RsrA, Zn−RsrA H37A, Zn−RsrA^{C11,C41,C44}) was shown by PAR assay to be ~1 mol equiv/RsrA (data not shown). We also assessed the function of these two mutants by their ability to bind σ^R in vitro (Figure 4).

EXAFS data for all Zn-loaded RsrA samples are shown in Figure 5 (insets) along with the Fourier transform data (main figure). Processed data for wild-type Zn−RsrA (Figure 5a) were fitted using two-shell simulations (red line) in which the primary shell comprised three sulfur atoms (main peak), with Zn−S distances of 2.33 Å, and a secondary shell (side-peak arrow) comprising one oxygen or nitrogen atom, with a Zn−O/N distance of 2.03 Å (see Materials and Methods for details). This second shell was included to take account of a clear shoulder on the main Zn−S peak in the Fourier transforms that cannot be modeled merely by sulfur coordination (Figure 5a). We used a statistical test that is part of the EXCURV98 program to determine whether the improvement in fit on addition of an extra shell justifies the extra parameters needed. The second shell did not in this case improve the statistics of the fit; however, since sulfur (high-Z) backscattering dominates EXAFS [and in many instances obscures the nitrogen/oxygen (low-Z) backscattering] (*34*), this was not surprising. As described below, the shoulder can clearly be assigned to a specific residue, and so all EXAFS data (with the exception of RsrA H37A mutant) were fitted according to two-shell simulations comprising three sulfurs and one nitrogen/oxygen atom.

All fitted parameters obtained from these simulations as well as those for fits to a single shell are shown in Table 1. Wild-type Zn−RsrA Zn K-edge EXAFS data are consistent with both models that have been proposed thus far, where three cysteines and a histidine residue are predicted to comprise the metal-binding site. However, EXAFS data for the Zn−RsrA^{C11,C41,C44} mutant (Figure 5b), where the four nonessential cysteine residues (Cys3, Cys31, Cys61, and Cys62) are substituted to alanine but Cys11, Cys41, and Cys44 are retained, clearly differentiate between the models since the data are essentially the same in phase and amplitude to those of wild-type Zn−RsrA. Hence, the coordination chemistry of the Zn^{2+} ion proposed by Li et al. comprising

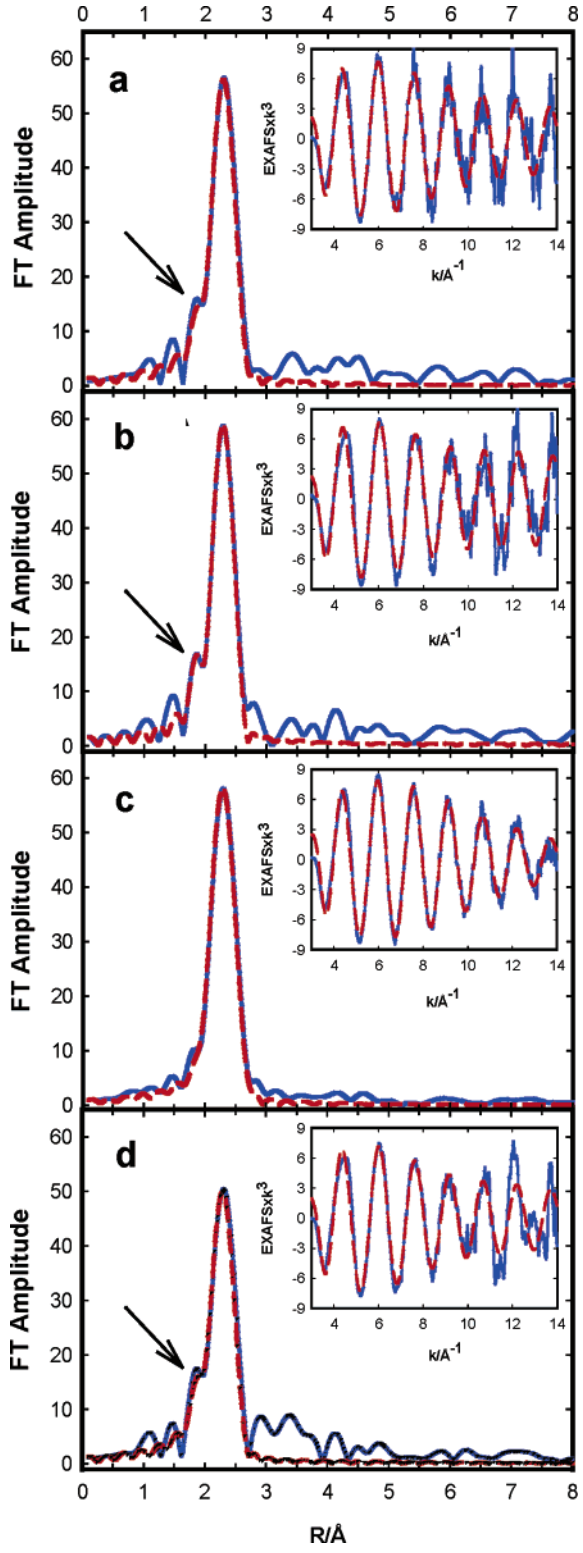

FIGURE 5: k^3-weighted EXAFS data (inset) and Fourier transform data (main panels) of Zn−RsrA in 50 mM Tris-HCl, pH 7.5, 200 mM NaCl, and 20 mM DTT. Panels: (a) wild-type Zn−RsrA; (b) Zn−RsrA^{C11,C41,C44}; (c) Zn−RsrA H37A; (d) wild-type Zn−RsrA bound to the sigma factor σ^R. Traces: blue, raw data for all samples; red, fit to raw data. In the case of wild-type ($\pm\sigma^R$) and Zn−RsrA^{C11,C41,C44} (panels a, b, and d), the fit was to a primary ligation shell of three sulfur atoms (main peak) and one N/O atom. In the case of Zn−RsrA H37A (panel c), the fit was to a primary ligation shell of four sulfur atoms. The arrow indicates the position of the Zn−N spectral feature that disappeared when His37 was mutated to alanine. All EXAFS data are collated in Table 1.

Table 1: Comparison of Various Fits to the EXAFS Data of Wild-Type Zn−RsrA, the RsrA^{C11,C41,C44} and RsrA H37A Mutants, and the Complex of Zn−RsrA with σ^R [a]

	Zn−S			Zn−N				
sample	*n*	*R* (Å)	$2\sigma^2$ (Å)	*n*	*R* (Å)	$2\sigma^2$ (Å)	*R*	χ^2 (10^{-6})
WT RsrA	3	2.33	0.006				38.5	4.49
	3.7	2.33	0.008				35.6	4.41
	3.0	*2.33*	*0.006*	*1.0*	*2.03*	*0.008*	*33.7*	*7.04*
	3.3	2.32	0.007	0.8	2.01	0.005	33.6	7.01
RsrA^{C11,C41,C44}	3.0	2.31	0.005				35.3	3.85
	3.4	2.31	0.007				33.7	3.74
	3.0	*2.31*	*0.005*	*1.0*	*2.00*	*0.003*	*31.1*	*5.61*
	3.5	2.31	0.008	0.7	1.98	0.001	30.9	5.64
RsrA H37A	4.1	2.33	*0.009*				17.6	0.97
RsrA−σ^R	3	2.32	0.007				41.0	5.02
	3.6	2.32	0.010				39.0	4.83
	3	*2.32*	*0.007*	*1.0*	*2.02*	*0.005*	33.6	*7.00*
	2.9	2.32	0.007	1.2	2.02	0.007	33.5	6.98

[a] *n* is the number of scatterers ± 15% (inner shell) ± 25% (outer shell); *r* is the Zn−scatterer distance ± 0.02 Å (inner shell) ± 0.05 Å (outer shell); $2\sigma^2$ is the Debye−Waller factor ± 15% (inner shell) ± 25% (outer shell). Italicized numbers represent the best fits to the data based on a two-shell fit of three sulfurs and one nitrogen. Only RsrA H37A did not conform to this model (see text for details).

cysteines at positions 11, 41, and 44 is correct (*1*). This model also suggested that His37 was a metal ligand. This is now confirmed by the EXAFS data for the H37A Zn−RsrA mutant, where the side peak in the Fourier transform data modeled as N or O at 2.03 Å disappeared (Figure 5c). The number of scatterers points to 4.1 sulfur atoms at 2.33 Å, which implies more sulfurs on average are coordinated in this mutant (Table 1). However, it is impossible to verify whether this additional sulfur is coordinated in RsrA H37A as a result of inter- or intramolecular interaction. Finally, we analyzed the influence of sigma factor binding on the Zn K-edge EXAFS spectrum of wild-type Zn−RsrA to determine whether this affected metal ion coordination (Figure 5d). No change was seen in the main EXAFS peaks <3 Å from the metal ion from which we conclude that the metal ligands in Zn−RsrA do not change when the anti-sigma factor is bound to σ^R. Nevertheless, additional scattering was evident between 3 and 4 Å, which could simply be an increase in spectrum noise or might represent a conformational change in Zn−RsrA that is induced by the sigma factor.

DISCUSSION

Model of the Metal Site in RsrA: Implications for Zinc-Mediated Redox Sensing in ZAS Proteins. Our mutagenesis and EXAFS data together show that the single zinc atom of the ZAS protein RsrA is ligated by Cys11, His37, Cys41, and Cys44. A mutant of RsrA where the remaining cysteines had been removed, including one central to the zinc-ligation model of Bae et al. (*33*), shows wild-type redox-sensing behavior in vivo (*17*) and an EXAFS spectrum identical to that of the wild-type protein. The importance of His37 and its involvement in the ligation of the metal ion was confirmed by its repeated isolation in random mutagenesis screens and the loss of the discernible shoulder in the EXAFS spectrum for H37A RsrA (Figure 5). The EXAFS spectrum for Zn−RsrA is typical of zinc metalloproteins where the metal ion is tetrahedrally coordinated by one nitrogen and three sulfur atoms (*35*). The spectroscopic data also show that binding of the sigma factor σ^R does not cause a change in metal-ligation chemistry (Figure 5d).

Our data confirm that the redox switch that modulates RsrA activity involves two of its four zinc ligands, Cys11 and Cys44, which explains why the metal ion is expelled during oxidation. Formation of this first disulfide causes a major restructuring of RsrA (*1*), resulting in its dissociation from σ^R and activation of its regulon to counteract the disulfide stress being experienced by the cell. Although Cys11 preferentially forms a trigger disulfide with Cys44, it can also, to a lesser extent, form a disulfide with Cys41, the other metal ligand of the ZAS motif (*1*, *33*). It is likely that these disulfides can oxidize other cysteines in the protein through thiol−disulfide exchange. Consistent with this, Bae et al. have identified an additional disulfide bond between residues 41 and 61 that forms in addition to the Cys11−Cys44 disulfide (*33*). Ultimately, fully oxidized RsrA contains three disulfide bonds (*16*). The behavior of the Zn−RsrA H37A is surprising in terms of its different ability to bind σ^R in vitro and its functionality in vivo. Whereas Zn−RsrA H37A is able to bind zinc and form a complex with its target transcription factor in vitro (Figure 4), the mutant is completely inactive in vivo (Figure 2). The same is also true of alanine mutations at any of the three cysteine ligands of the zinc ion (*17*). This could be because mutants at ZAS residues render the protein sensitive to proteolytic degradation or are unable to bind zinc tightly, making them more prone to oxidation and hence inactivation in vivo. Either outcome would yield the constitutive σ^R transcriptional activities observed for strains of *Streptomyces* carrying these mutations (*17*).

Assuming that each member of the ZAS family possesses a zinc-binding domain of similar overall structure to that of RsrA, this raises an important question: why do not all ZAS proteins exhibit a similar redox switch? A comparison of the primary sequence of RsrA and ChrR suggests one possible explanation. ChrR lacks Cys11 but instead has two histidine residues close to this position (Figure 1), one of which might act in concert with the HxxxCxxC motif to coordinate zinc. Thus, ChrR is not able to form the equivalent Cys11−Cys44 disulfide bond, providing a possible explanation as to why ChrR is not responsive to diamide or hydrogen peroxide. The ability of ChrR to sense singlet oxygen presumably involves a region that is unique to this protein. The apparent inability of RsiW to sense redox signals is not easily explained. Together with its invariant HxxxCxxC motif, RsiW has a cysteine at a position equivalent to Cys11 in RsrA (Figure 1) and yet does not appear to respond to oxidants. Rather, it is proposed that the cytoplasmic N-terminal ZAS domain releases σ^W following intramembrane proteolysis of RsiW in response to an extracellular signal sensed by its C-terminal extracytoplasmic domain (*18*). This implies that the presence of a cysteine at a position equivalent to Cys11 in RsrA is necessary but not sufficient for an RsrA-like mechanism of redox sensing but that the involvement of the zinc ligands in redox sensing in RsrA might be atypical among ZAS proteins. If this is the case, it suggests that the zinc-binding domain of RsrA has evolved from a purely structural domain to one with a combined structural/redox-sensing ability. The precise feature(s) of RsrA that distinguish

it from non-redox-sensing ZAS proteins remain(s) to be discerned.

ACKNOWLEDGMENT

We thank Robert Bilsborrow for technical assistance during data collection at SRS Daresbury Laboratory, John Charnock and Richard Strange for help with interpretation of EXAFS results, and Jan Dohnalek for computer support.

REFERENCES

1. Li, W., Bottrill, A. R., Bibb, M. J., Buttner, M. J., Paget, M. S., and Kleanthous, C. (2003) The role of zinc in the disulfide stress-regulated anti-sigma factor RsrA from *S. coelicolor*, *J. Mol. Biol. 333*, 461−472.
2. Halliwell, B., and Gutteridge, J. C. (1999) *Free radicals in biology and medicine*, Oxford University Press, New York.
3. Nakamura, H., Nakamura, K., and Yodoi, J. (1997) Redox regulation of cellular activation, *Annu. Rev. Immunol. 15*, 351−369.
4. Ritz, D., and Beckwith, J. (2001) Roles of thiol-redox pathways in bacteria, *Annu. Rev. Microbiol. 55*, 21−48.
5. Åslund, F., and Beckwith, J. (1999) Bridge over troubled waters: sensing stress by disulfide bond formation, *Cell 96*, 751−753.
6. Georgiou, G. (2002) How to flip the (redox) switch, *Cell 111*, 607−610.
7. Paget, M. S. B., and Buttner, M. J. (2003) Thiol-based regulatory switches, *Annu. Rev. Genet. 37*, 91−121.
8. Zheng, M., Aslund, F., and Storz, G. (1998) Activation of the OxyR transcription factor by reversible disulfide bond formation, *Science 279*, 1718−1721.
9. Choi, H., Kim, S., Mukhopadhyay, P., Cho, S., Woo, J., Storz, G., and Ryu, S. (2001) Structural basis of the redox switch in the OxyR transcription factor, *Cell 105*, 103−113.
10. Lee, C., Lee, S. M., Mukhopadhyay, P., Kim, S. J., Lee, S. C., Ahn, W. S., Yu, M. H., Storz, G., and Ryu, S. E. (2004) Redox regulation of OxyR requires specific disulfide bond formation involving a rapid kinetic reaction path, *Nat. Struct. Mol. Biol. 11*, 1179−1185.
11. Ilbert, M., Graf, P. C. F., and Jakob, U. (2006) Zinc Center as redox switch—new function for an old motif, *Antioxid. Redox Signaling* (in press).
12. Jacob, U., Eser, M., and Bardwell, J. C. (2000) Redox switch of Hsp33 has a novel zinc-binding motif, *J. Biol. Chem. 275*, 38302−38310.
13. Maret, W. (2004) Zinc and sulfur: A critical biological partnership, *Biochemistry 43*, 3301−3309.
14. Paget, M. S., Kang, J. G., Roe, J. H., and Buttner, M. J. (1998) sigmaR, an RNA polymerase sigma factor that modulates expression of the thioredoxin system in response to oxidative stress in *Streptomyces coelicolor* A3(2), *EMBO J. 17*, 5776−5782.
15. Paget, M. S. B., Molle, V., Cohen, G., Aharonowitz, Y., and Buttner, M. J. (2001) Defining the disulphide stress response in *Streptomyces coelicolor* A3(2): identification of the σ^R regulon, *Mol. Microbiol. 42*, 1007−1020.
16. Kang, J. G., Paget, M. S., Seok, Y. J., Hahn, M. Y., Bae, J. B., Hahn, J. S., Kleanthous, C., Buttner, M. J., and Roe, J. H. (1999) RsrA, an anti-sigma factor regulated by redox change, *EMBO J. 18*, 4292−4298.
17. Paget, M. S. B., Bae, J.-B., Hahn, M.-Y., Li, W., Kleanthous, C., Roe, J.-H., and Buttner, M. J. (2001) Mutational analysis of RsrA, a zinc-binding anti-sigma factor with a thiol-disulphide redox switch, *Mol. Microbiol. 39*, 1036−1047.
18. Schobel, S., Zellmeier, S., Schumann, W., and Wiegert, T. (2004) The *Bacillus subtilis* σ^W anti-sigma factor RsiW is degraded by intramembrane proteolysis through YluC, *Mol. Microbiol. 52*, 1091−1105.
19. Wiegert, T., Homuth, G., Versteeg, S., and Schumann, W. (2001) Alkaline shock induces the *Bacillus subtilis* σ^W regulon, *Mol. Microbiol. 41*, 59−71.
20. Cao, M., Wang, T., Ye, R., and Helmann, J. D. (2002) Antibiotics that inhibit cell wall biosynthesis induce expression of the *Bacillus subtilis* σ^W and σ^M regulons, *Mol. Microbiol. 45*, 1267−1276.
21. Newman, J. D., Anthony J. R., and Donohue T. J. (2001) The importance of zinc-binding to the function of *Rhodobacter sphaeroides* ChrR as an anti-sigma factor, *J. Mol. Biol. 313*, 485−499.
22. Anthony, J. R., Warczak, K. L., and Donohue, T. J. (2005) A transcriptional response to singlet oxygen, a toxic byproduct of photosynthesis, *Proc. Natl. Acad. Sci. U.S.A. 102*, 6502−6507.
23. Kieser, T., Bibb, M. J., Buttner, M. J., Chater, K. F., and Hopwood, D. A. (2000) *Practical Streptomyces Genetics*, The John Innes Foundation, Norwich.
24. Paget, M. S., Chamberlin, L., Atrih, A., Foster, S. J., and Buttner, M. J. (1999) Evidence that the extracytoplasmic function sigma factor sigmaE is required for normal cell wall structure in *Streptomyces coelicolor* A3(2), *J. Bacteriol. 181*, 204−211.
25. Bierman, M., Logan, R., O'Brien, K., Seno, E. T., Rao, R. N., and Schoner, B. E. (1992) Plasmid cloning vectors for the conjugal transfer of DNA from *Escherichia coli* to *Streptomyces* spp., *Gene 116*, 43−49.
26. Ward, J. M., Janssen, G. R., Kieser, T., Bibb, M. J., and Buttner, M. J. (1986) Construction and characterisation of a series of multi-copy promoter-probe plasmid vectors for *Streptomyces* using the aminoglycoside phosphotransferase gene from Tn5 as indicator, *Mol. Gen. Genet. 203*, 468−478.
27. Fisher, C. L., and Pei, G. K. (1997) Modification of a PCR-based site-directed mutagenesis method, *BioTechniques 23*, 570−571, 574.
28. Li, W., Stevenson, C. E. M., Burton, N., Jakimowicz, P., Paget, M. S. B., Buttner, M. J., Lawson, D. M., and Kleanthous, C. (2002) Identification and structure of the anti-sigma factor-binding domain of the disulfide-stress regulated sigma factor SigR from *Streptomyces coelicolor*, *J. Mol. Biol. 323*, 225−236.
29. Ellis, P. (1995) Ph.D. Thesis, University of Sydney, NSW, Australia.
30. Binsted, N. (1998) EXCURV98: CCLRC, Daresbury Laboratory computer program.
31. Gurman, S. J., Binsted, N., and Ross, I. (1984) A rapid, exact curved-wave theory for EXAFS calculations, *J. Phys. C 17*, 143−151.
32. Hedin, L., and Lundqvist, S. (1969) Effects of electron-electron and electron-phonon interactions on the one-electron states of solids, *Solid State Phys. 23*, 1−181.
33. Bae, J. B., Park, J. H., Hahn, M. Y., Kim, M. S., and Roe, J. H. (2004) Redox-dependent changes in RsrA, an anti-sigma factor in *Streptomyces coelicolor*: zinc release and disulfide bond formation, *J. Mol. Biol. 335*, 425−435.
34. Clark-Baldwin, K., Tierney, D. L., Govindaswamy, N., Gruff, E. S., Kim, C., Berg, J., Koch, S. A., and Penner-Hahn, J. E. (1998) The limitations of X-ray absorption spectroscopy for determining the structure of zinc sites in proteins. When is a tetrathiolate not a tetrathiolate?, *J. Am. Chem. Soc. 120*, 8401−8409.
35. Summers, M. F., Henderson, L. E., Chance, M. R., Bess, J. W., South, T. L., Blake, P. R., Sagi, R., Perez-Alvarado, G., Sowder, R. C., III, Hare, D. R., and Arthur, L. O. (1992) Nucleocapsid zinc fingers detected in retroviruses: EXAFS studies of intact viruses and the solution-state structure of the nucleocapsid protein from HIV-1, *Protein Sci. 1*, 563−574.

BI060711V